Proceedings of the National Conference
On Undergraduate Research (NCUR) 2016
University of North Carolina at Asheville
Asheville North Carolina
April 7-9, 2016

Combustion-Cylinder Optimization for an Active Ankle-Foot Orthosis

Sarah Swanson
Mechanical and Industrial Engineering
Montana State University – Bozeman
201 Strand Union Building
Bozeman, Montana 59717 USA

Fluid Power Institute™
Milwaukee School of Engineering
1025 N. Broadway
Milwaukee, WI 53202

Faculty Advisor: Douglas Cook

Abstract

Working from a previously-synthesized design concept, this research focuses on the optimization of a spark-ignition, internal-combustion actuator, intended to provide direct actuation for ankle plantarflexion in an active ankle-foot orthosis (AAFO). Optimization of the cylinder design was focused on meeting pressure and force loading requirements, through the gas-power cycle. Both, the designable (dynamic design space) and non-designable (fixed) geometries were generated using SolidWorks®, and were then imported into solidThinking Inspire® for optimization. The fixed geometry was used for load applications, and to establish certain necessary design features. Dynamic design space was created around the fixed geometry, within which the software algorithm performed its morphological optimization process, dependent on the connections and setup specified. In order to establish the loads for the setup, it was necessary to correlate the gait cycle to the power cycle, and determine the pressure-volume relationship for the design. The desired result was a combustion-cylinder design optimized for the projected loading during the power cycle required to provide full gait assistance. Future work will include the thermal-management requirements in the cylinder optimization. These include, but are not limited to, external surface temperature, as mandated by the Food and Drug Administration (FDA), flame quenching considerations, and further material considerations.

Keywords: AFO, Internal Combustion, Optimization

1. Introduction

Human gait has been studied for decades. Observation indicates that, although the gait cycle varies between individuals and conditions, the qualitative nature is consistent for healthy individuals. A pathological gait is a gait that deviates from this qualitative standard in some fashion. In the United States alone, more than six million individuals suffer from a disease or injury resulting in a pathological gait[1]. These individuals are potential candidates for an ankle-foot orthosis (AFO).

The AFOs currently available are considered to be passive because they do not integrate any active actuation or electronic control elements[2,3]. Designs range from fully-rigid, non-articulated AFOs to articulated AFOs that incorporate hinges and stiffness-control components[4]. Regardless of design, the devices are intended to provide ankle and foot support and alignment, while allowing for various degrees of joint motion. The fully-rigid, non-articulated AFOs serve to immobilize a patient's ankle joint. A less-rigid, non-articulated AFO may be designed to act more as a leaf spring that releases stored potential energy during the pre-swing push-off[4]. Articulated devices allow for passively-controlled motion in the sagittal plane. These designs generally allow for freedom of motion for dorsiflexion, while resisting plantarflexion to prevent the occurrence of drop-foot[4]. Although articulated passive AFOs are a theoretical improvement over the non-articulated models, introducing active elements provides the potential for variable control based on active gait-event feedback[1]. The investigation of using an untethered power source for an active AFO (AAFO) is intended to increase the possibilities of assisting individuals with pathological gaits in their everyday lives.

1.2 Developing and Existing Technologies

There are a wide variety of passive AFOs in production, but published literature indicates that there are not any commercially-available, autonomous AAFO designs[2,3]. In order to understand the requirements for an AAFO, it is important to develop a general understanding of some of the available and developing active and passive AFO technologies.

1.2.1 intrepid dynamic exoskeletal orthosis

The Intrepid Dynamic Exoskeletal Orthosis (IDEO) is a passive AFO invented by Ryan Blanck in 2009, while working for the Center for the Intrepid (CFI) at Brooke Army Medical Center, Fort Sam Houston, Texas[5]. The device is designed to store and release energy, analogous to a leaf spring, and allows its wearer to walk, run and sprint over a variety of terrains[5]. As of 2013, over 460 military limb-salvage patients, including those in special operations, were able to return to duty, and even combat, because of the IDEO[5]. However, despite the apparent advantages of the device, particularly for an active demographic, it does have the inherent limitations of a passive AFO. The IDEO is also only available at the CFI; although, there are thoughts of expanding its availability to other Army rehab centers and, eventually, to the civilian population[5].

1.2.2 active, soft, ankle-foot orthosis

A team from Harvard presented an active, soft, AFO at the 2011 IEEE/RSJ International Conference on Intelligent Robots and Systems[6]. This was one of the few active AFOs, that the author found, that was not developed in association with the Center for Compact and Efficient Fluid Power (CCEFP). The design is unique, not only for its use of soft components, but also because it provides control in both sagittal and mediolateral ankle motions[6]. This potentially allows a patient to have a range of motion more similar to that of a healthy individual. No information was found regarding the mass of the AFO. In regards to run time, the electronics could run for several hours off of batteries, but the pneumatics still required a line connection, so the device could not be used untethered[6].

1.2.3 previous ccefp projects

CCEFP has previously supported AAFO research and development as part of the center's Test Bed 6, involving human-assist devices. The focus of this test bed is to develop human-scale, untethered, fluid-power devices, in an effort to determine if the energy-to-weight and power-to-weight advantages of fluid-power systems are maintained for small-scale, low-power devices[7]. AAFOs are being used as the platform for the fluid-power actuators.

In 2009 the University of Minnesota presented a free-piston-engine-driven compressor, designed to be small enough to attach to the posterior side of the AAFO, at the Small Engine Technology Conference in Penang, Malaysia. Due to the greater power density of hydrocarbon fuel, the device was able to exceed the power density of a battery-run actuator; but, at a predicted system efficiency of 5.9%, there is room for improvement[8].

In 2011 a team at the University of Illinois presented a full AAFO prototype, powered off of a cylinder of compressed carbon dioxide. The design had a total mass of 3.1 kg, with 1.9 kg comprising the orthosis components, and the remainder consisting of the compressed CO_2 canister and regulator attached at the waist[3]. The target is to add less than one kilogram of mass to the affected limb, in this case, the lower leg[7]. The result is that the design is 0.9 kg (90%) over target. The amount of compressed CO_2 required for a full day of operation was not published, but it was noted that replenishing the canisters does pose a logistical obstacle to the design[3].

1.2.4 additive-manufacturing customization

Additive-manufacturing (AM) allows for greater geometric design freedom than traditional manufacturing processes. The translation of impression casts, or three-dimensional scans, to computer-aided-design (CAD) models allows for the generation of an orthosis specific to a patient's anatomy (bespoke orthotics). A variety of AFOs have been generated using AM, but most of the designs have not deviated significantly from those manufactured using traditional processes[9]. However, some designs have emerged that would take advantage of the flexibility provided by AM, and incorporate features, particularly related to adjustability, that would be otherwise difficult to include[9].

1.3 System Design Concept

One of the challenges in developing untethered, powered orthotics is integrating a suitable energy source[2]. This challenge drives the exploration of a myriad of different actuator types. This project focuses on the structural optimization of a spark-ignition, combustion-driven actuator for plantarflexion assistance. The concept utilizes the combustion cylinder as a primary actuator for plantarflexion, and incorporates a secondary pneumatic actuator to operate off of the combustion-cylinder exhaust, assisting in dorsiflexion. Due to the forced induction, overexpansion potential, energy-harvesting mechanisms, and exhaust-energy recovery, integrated into the concept, the system is estimated to have a theoretical thermodynamic efficiency greater than 60%[10,11]. Optimizing the structural design of the combustion-cylinder will contribute to the mass minimization of the overall system, while maintaining structural integrity for the safety of a potential AAFO patient.

2. Methodology

As it is desirable that an AAFO would provide assistance to its wearer without adding significant mass to the wearer's lower limb, it is important to minimize the mass of the device's individual components, without compromising safety or functionality. The following outlines the assumptions, and other processes, used to optimize a combustion-driven actuator that would use a combination of additive and traditional manufacturing techniques for construction.

2.1 Derivation of Assumptions

In order to complete the design and optimization of the combustion-cylinder, it was necessary to set certain design specifications, and establish a set of assumptions. Initial values for the cylinder bore (b = 2.54 cm) and the maximum desired system pressure (35 bar) were provided as a baseline. A design parameter of a maximum 7.62 cm cylinder housing diameter was also provided. The initial cylinder bore dimension was arbitrarily held constant to establish a value from which other parameters could be derived.

One of the underlying assumptions for this AAFO system concept is that it would be capable of providing full compensation for normal ankle torques. This required the establishment of what normal ankle torques would be considered. A gait lab was not available in which a normative study could be performed, so it was decided to accept the values published in David A. Winter's book *Biomechanics and Motor Control of Human Movement* as standards.

It was next assumed that the system would use a fixed-diameter pulley to translate the linear piston motion into the rotary motion required to achieve plantarflexion. The cylinder bore and maximum ankle torque (τ_{max} = 90 N·m)[12] were used to correlate maximum pressure (P_{max} = 35.5 bar) and pulley diameter (d_p = 10 cm), and to set the listed values for both using equation (1). The finalized maximum pressure and pulley diameter values resulted in a maximum ankle torque of 89.94 N·m, which is within 0.1% of the approximated maximum torque value required for full torque compensation.

$$\tau_{max}/(P_{max}\cdot\pi * b^2/4) = d_p/2 \qquad (1)$$

An arbitrary hydrocarbon fuel, n-butane, was selected for the purposes of establishing a theoretical gas-power cycle. These calculations assumed a limited-pressure cycle operating with ideal-gas mixtures[13]. The volumes for the cycle were derived from the angular motion of the ankle. The values listed in *Biomechanics and Motor Control of Human Movement* were again considered to be normative. It is further assumed that the intake stroke occurs under forced induction conditions, with the pressure equivalent to the vapor pressure of n-butane[10]. This value was calculated using the Antoine equation, equation (2), where P is vapor pressure in bar and T is temperature in Kelvin.

$$\log_{10}(P) = A - (B / (T + C)) \tag{2}$$

The relevant values for parameters A, B and C are listed in Table 1 below.

Table 1. Antoine equation parameters (table adapted from)[14]

Temperature (K)	A	B	C
272.66 – 425.00	4.35576	1175.581	-2.071

The use of equation (2), with the parameters listed in Table 1 and an inlet temperature of 25 °C (T = 298.15 K), resulted in the vapor pressure of n-butane being calculated as 2.43 bar[14].

The cylinder was initially assumed to be primarily constructed of a plastic material on a Selective Laser Sintering (SLS) 3D printer. The plastic was to be shielded from direct contact with the combustion gases by a thin steel liner of arbitrary thickness (0.0254 cm). This design also incorporated a spark plug, assumed to be a Rimfire Micro Viper Z3, the only commercially-available spark plug of an appropriate size that the author could identify, and valves. All of the valves were represented by simple approximated geometry, because; suitable valves were not found to be commercially available, and there was insufficient time to fully develop the valves.

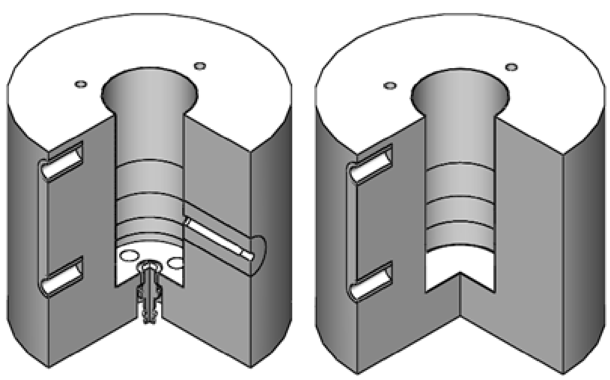

Figure 1. Comparison of complex and simplified pre-optimization geometries

The geometry shown on the left in Figure 1 above is the initial geometry created for import into the optimization software. This initial geometry included the spark plug and simple valve geometries. The geometry shown on the right in Figure 1 is a simplified geometry that was ultimately used due to computer-processing-power and software limitations. The final geometry used was further simplified by assuming that all of the material was aluminum. This was deemed necessary after initial trial optimizations, using multiple materials, failed to complete.

2.2 Optimization Process

Prior to optimization, a base design had to be finalized for the non-designable (fixed) geometries. This fixed geometry was necessary for the application of loads, the establishment of connection points, and to locate critical elements. Designable (dynamic design space) geometry was created around the fixed geometry to fill the 7.62 cm diameter space permitted for the cylinder housing. The geometry was all generated in SolidWorks®, and then imported into solidThinking Inspire® for mass optimization.

There is a limited materials library database included in solidThinking Inspire®. In order to avoid potential errors due to non-natively defined materials, all components were assigned materials from the provided library. Initial trial runs assigned the dynamic design space and bracket to a Nylon material, whereas the remaining geometry was assigned to be AISI 316 steel. After these trial runs and various other material settings were unsuccessful, the geometry was ultimately set entirely to 6061 aluminum.

Following the definition of geometry and material properties, the geometry was constrained and load cases were established. The model was assumed to be fixed in the two bracket holes, where the cylinder would attach to the orthosis shell. The load cases were established based off of the pressure-volume diagram, derived from the power-cycle calculations. Three volumes were matched with the maximum corresponding pressures to imitate the gradient of pressures that would occur along the cylinder wall during combustion.

3. Results

3.1 Power Cycle

The load cases for the optimization were selected from the expansion portion of the power cycle developed for the combustion-cylinder, shown in Figure 2. The highest pressure case, at phase 6, was selected as the first load case. The second load case was established at a volume equivalent to that at phase 3, but at the pressure occurring on the expansion stroke. The final load case was selected to correspond to phase 7. The load cases were applied by dividing the cylinder liner into rings that ended at locations corresponding to the appropriate volumes. The n-butane power-cycle values are presented in Table 2**Error! Reference source not found.**.

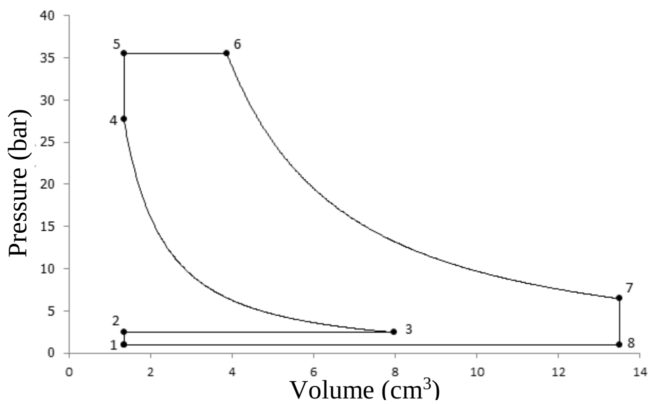

Figure 2. n-butane limited-pressure model power cycle

Table 2. n-butane power-cycle values

	Pressure [bar]	Temperature [K]	Volume [cm^3]	n [10^{-4} mol]
1	1.013	298.15	1.351	0.552
2	2.428	298.15	1.351	1.32
3	2.428	298.15	7.984	7.82
4	27.69	575.30	2.666	7.82
5	35.50	737.70	2.666	7.82
(Load Case 1) 6	35.50	2117.8	3.879	7.82
(Load Case 2)	13.21	1621.5	7.984	7.82
(Load Case 3) 7	6.422	1334.6	13.51	7.82
8	1.013	210.56	13.51	7.82

3.2 Optimized Geometry

Due to time constraints, it was deemed prudent to focus on a single optimization program, solidThinking Inspire®, to get results. The initial geometry addressed in the methodology did not return any results, even when material properties were adjusted. It was then decided that the geometry was too complex for solidThinking Inspire® to feasibly mesh and analyze. As a result, the pre-optimization geometry was simplified down to the second geometry addressed in the methodology.

Even with a simplified geometry and material definition, solidThinking Inspire® failed to confirm an optimized resultant geometry. It is unclear as to whether the lack of an optimized geometry was due to computational power of the computer used, faulty setup parameters, or a problem with the software itself. However, even though an optimized geometry was not confirmed, a low-mass modified geometry was produced that satisfied a minimum safety factor of 1.2 for all three load cases applied.

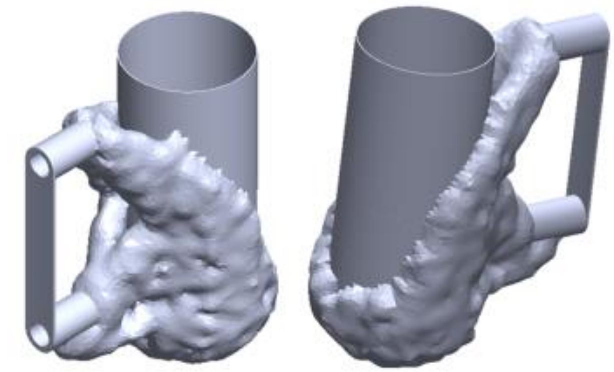

Figure 3. Low-mass geometry generated in solidThinking Inspire®

The low-mass geometry mentioned previously is shown in Figure 3, and is representative of the type of qualitative characteristics that might be expected in an optimized geometry. Rather than utilizing the simple forms desirable for traditional manufacturing processes, the solid-isotropic-material-with-penalization (SIMP) optimization method employed by solidThinking Inspire® returns an organic shape more suitable to additive manufacturing.

In order to further explore the results produced by solidThinking Inspire®, it was attempted to import the geometry into a separate finite-element-analysis (FEA) software for analysis. The geometry could not be analyzed in ANSYS®, because the author was unable to generate a satisfactory mesh. An attempt was also made to use COMSOL Multiphysics® for this secondary analysis. Although COMSOL ultimately generated a satisfactory mesh of the geometry, it was unable to converge on the solution for the analysis. This meant that it was not possible to corroborate the analysis results generated in solidThinking Inspire®, as the secondary software analyses were unsuccessful, and the geometry was too abstract for analysis by hand calculations.

Although the geometry was not optimized, a mass comparison was made with an off-the-shelf pneumatic cylinder to evaluate the potential for mass reduction. In order to make a fair comparison between the two geometries, the piston, valves, and other components not yet integrated into the low-mass geometry were not included in the mass estimate for the off-the-shelf cylinder. The low-mass cylinder was estimated to have a mass of 49.39 g compared to 224.5 g for an arbitrary off-the-shelf cylinder. This represents a 78 percent reduction in mass from the off-the-shelf cylinder to the low-mass geometry generated in solidThinking Inspire®. The comparison does not take into account the difference in safety factors between the two cylinders, in part because the safety factor for the off-the-shelf cylinder is not known for the given application. However, with appropriately selected materials and the use of optimization, there appears to be the potential for significant mass reduction over the off-the-shelf cylinder.

4. Recommendations

Future work concerning the optimization of a combustion actuator for an AAFO could improve upon the parameters used in this research. The pressure loadings applied for the optimization should be validated through the establishment of a real gas cycle for n-butane. This should assist in the identification of all pressure cases not accounted for by the limited-pressure cycle approximation. The load cases could also be adjusted to account for frictional forces between the piston and the cylinder wall. The analysis could be further extended to account for the running gait cycle. Research conducted indicated the availability of qualitative running gait cycle information, however, normative quantitative data was not found. Accounting for the running gait cycle would grant the potential for the AAFO to be used for a wider variety of activities.

Furthermore, future work should take into account a variety of additional factors. In terms of the cylinder properties, consideration should be for specific material selection, valve and spark plug placement, and piston design.

5. Conclusion

Due to time and software limitations, an optimized geometry was not confirmed for this combustion-cylinder. Following iterative adjustment of settings in solidThinking Inspire®, it remained uncertain as to the root cause for not achieving an optimized configuration. However, the research does indicate that, when the root cause is identified, the cylinder optimization has the potential for significant mass reduction over off-the-shelf-pneumatic cylinders. This is critical for minimizing the mass of the overall AAFO. Once an optimization procedure is validated, future work could take into account improved load cases, the running gait cycle, and design specifics.

6. Acknowledgements

This material is based upon work supported by the National Science Foundation under Grant No. EEC-0540834. Any opinions, findings, and conclusions or recommendations expressed in this material are those of the author(s) and do not necessarily reflect the views of the National Science Foundation.

The author would like to thank the Fluid Power Institute™ for the additional funding provided for this project. Special thanks to Douglas Cook (advisor), Dr. Subha Kumpaty, Betty Albrecht, and the other MSOE faculty and staff that supported this endeavor.

7. References

1. David Yifan Li et al., "Estimating System State During Human Walking With a Powered Ankle-Foot Orthosis," *IEEE/ASME Transactions on Mechatronics* 16, no.5 (October 2011): 835-844, doi: 10.1109/TMECH.2011.2161769.

2. Aaron M. Dollar and Hugh Herr, "Lower Extremity Exoskeletons and Active Orthoses: Challenges and State-of-the-Art," *IEEE Transactions on Robotics* 24 no. 1 (February 2008): 144-158, doi: 10.1109/TRO.2008.915453.

3. K. Alex Shorter et al., "A Portable Powered Ankle-Foot Orthosis for Rehabilitation," *Journal of Rehabilitation Research and Development* 48 (2011): 459-472, doi: 10.1682/JRRD.2010.04.0054.

4. Morshed Alam, Imtiaz Ahmed Choudhury and Azuddin Bin Mamat, "Mechanism and Design Analysis of Articulated Ankle Foot Orthoses for Drop-Foot," *The Scientific World Journal* (2014): n.p., doi: 10.1155/2014/867869.

5. David Vergun, "Device Gets Soldiers Back to Work on Their Feet, Preventing Amputations," United States Army, Last modified August 16, 2013, http://www.army.mil/article/109400/.

6. Yong-Lae Park et al., "Bio-inspired Active Soft Orthotic Device for Ankle Foot Pathologies," (paper presented at the IEEE/RSJ International Conference on Intelligent Robots and Systems, San Francisco, CA, September 25-30, 2011).

7. Elizabeth Hsiao-Wecksler, "Human Assist Devices – Fluid Powered Ankle Foot Orthosis (Test Bed 6)," Center for Compact and Efficient Fluid Power, Last modified 2015, http://www.ccefp.org/research/test-beds/fluid-powered-ankle-foot-orthosis.

8. Lei Tian, David B. Kittelson, William K. Durfee, "Miniature HCCI Free-Piston Engine Compressor For Orthosis Application," (paper presented at the Small Engine Technology Conference, Penang, Malaysia, November 3-5, 2009).

9. Scott Telfer et al., "Embracing Additive Manufacture: Implications for Foot and Ankle Orthosis Design," *BMC Musculoskeletal Disorders* 13, no. 84 (May 29, 2012): n.p., doi: 10.1186/1471-2474-13-84.

10. Douglas Lee Cook, "Actuation System for a Joint," US 2014/0260950 A1, filed March 13, 2014.

11. Douglas L. Cook, "Peak Force Measurements for a Combustion-Driven, Direct-Conversion, Actuation System for Powered Orthoses," Journal of Medical Devices 9, no. 2 (June 1, 2015): 020944, June 8, 2015. doi:10.1115/1.4030149.

12. David A. Winter, *Biomechanics and Motor Control of Human Movement* (New York: John Wiley & Sons, 1990), 254-256.

13. John B. Heywood, *Internal Combustion Engine Fundamentals* (New Yourk: McGraw-Hill, 1988), 163.

14. P. J. Linstrom and W. G. Mallard, "NIST Chemistry WebBook," National Institute of Standards and Technology, Last modified 2011, http://webbook.nist.gov.